SUPPORTING INFORMATION

pH-Sensitive Pt Nanocluster Assembly Overcomes Cisplatin Resistance and Heterogeneous Stemness of Hepatocellular Carcinoma

Hongping Xia,[†,§,⊥] Fangyuan Li,[†,‡,⊥] Xi Hu,[†,⊥] Wooram Park,[#] Shuaifei Wang,[†] Youngjin Jang,[∥,o] Yang Du,[†] Seungmin Baik,[∥,o] Soojeong Cho,[#] Taegyu Kang,[∥,o] Dong-Hyun Kim,[#,▽] Daishun Ling,*[,†,‡] Kam Man Hui,*[,§,◇] and Taeghwan Hyeon*[,∥,o]

[⊥] These authors contributed equally to this work.

* To whom correspondence should be addressed. E-mail: lingds@zju.edu.cn (D. L),cmrhkm@nccs.com.sg (K.M.H), thyeon@snu.ac.kr (T.H)

Methods and Materials

Materials. All of the solvents and chemical reagents were used as received from the commercial sources without further purification. $Pt(acac)_2$, super-hydride, oleylamine, oleic acid, 1-octadecene, octadecylamine, L-Aspartic acid β-benzyl ester, 1-(3-aminopropyl)imidazole (API), pluronic® F-127, 6-Maleimidohexanoic acid (MA), rhodamine B isothiocyanate (RITC), dicyclohexylcarbodiimide (DCC), 4-Dimethylaminopyridine (DMAP), *N*,*N*-Dimethylformamide, dichloromethane (DCM), tetrahydrofuran (THF), dimethyl sulfoxide (DMSO), were purchased from Sigma Chemical Company (St. Louis, MO). β-Benzyl-l-aspartate N-carboxy anhydride (BLA-NCA) was synthesized following our previous papers.[1,2]

Synthesis of Pt Nanoclusters. In order to synthesize the ultrasmall sized Pt nanoclusters, heat-up method was empolyed using thermal-decomposition of $Pt(acac)_2$ in the mixed solutions of oleylamine and oleic acid. The mixture was heated to 70 ^{o}C and stirred vigorously for 1 h under vacuum. After the mixture was heated to 170 ^{o}C, and 0.2 ml of super-hydride solution was injected, and was finally aged for 10 min to obtain uniform Pt nanocrystals.

Synthesis of the pH-Sensitive Peptide Ligand (Octadecylamine-p(API-Asp)$_{10}$). Octadecylamine-p(API-Asp)$_{10}$ was synthesized based on our previously reported methods.[2] β-Benzyl-l-aspartate N-carboxy anhydride (BLA-NCA; 3 g, 12 mmol) was polymerized in a mixture of dimethylformamide (DMF; 20 mL) and CH_2Cl_2 (50 mL) at 40°C by initiation from the terminal primary amino group of octadecylamine (MW = 269.51 g mol^{-1}, 0.3 g, 1.2 mmol). The reaction mixture was stirred for 2 days. CH_2Cl_2 solvent was removed by rotary evaporation. The polymer was precipitated in cold ethyl ether, and a white power was isolated by centrifugation (3500 rpm) for 5 min. pH-sensitive octadecylamine-p(API-Asp)$_{10}$ was

synthesized via aminolysis of the as-synthesized octadecylamine-PBLA with 1-(3-aminopropyl)imidazole (API). Octadecylamine-p(API-Asp)$_{10}$ (0.2, 74.8 μmol) was dissolved in anhydrous DMF (5 ml), followed by reaction with API (1 g, 7.9 mmol) under nitrogen at 25 °C and stirred for 12 h. The reaction mixture was added dropwise into a cooled aqueous solution of 0.1 N HCl (20 ml) and dialyzed against a 0.01 N HCl solution three times (Spectra/Por; MWCO: 1,000 Da) for 24 h. The final solution was lyophilized to obtain octadecylamine-p(API-Asp)$_{10}$ as a white solid, and production of octadecylamine-p(API-Asp)$_{10}$ was verified by proton nuclear magnetic resonance (^{1}H-NMR) spectroscopy.

^{1}H-NMR (500 MHz, DMSO-d$_6$) for octadecylamine–p(API-Asp)$_{10}$: δ = 7.8 ppm (1H, s, −NC<u>H</u>═N– of imidazole ring), 7.7 ppm (1H, s, −NC<u>H</u>═CH– of imidazole ring), 7.3 ppm (1H, s, −CH═C<u>H</u>–N– of imidazole ring), 4.5 ppm (1H, m,–NHC<u>H</u>C═O−), 4.0 ppm (2H, s, ═NC<u>H$_2$</u>CH$_2$), 3.0 ppm (2H, s, −NHC<u>H$_2$</u>CH$_2$−), 2.6 ppm (2H, m, −C<u>H$_2$</u>C═ONH−), 1.8 ppm (2H, s, −CH$_2$C<u>H$_2$</u>CH$_2$−), 1.2 ppm (17H, s, −C<u>H$_2$</u>– of octadecylamine), and 0.8 ppm (3H, t, C<u>H$_3$</u>– of octadecylamine).

Synthesis of Fluorescence-Labeled Peptide Ligands. pH-sensitive ligand or octadecylamine-PBLA, pH-insensitve ligand (100 mg) in DMSO (20 mL) was reacted with Rhodamine-B-Isothiocyanate (RITC) (30 mg) for 12 h at room temperature in the dark. The reaction mixture was dialyzed (MWCO: 1000 Da) for 2 days against distilled water to remove unlabeled RITC and DMSO.

Synthesis of 6-Maleimidohexanoic Acid-Pluronic F127 (MA-F127) Conjugates. Pluronic F127 powder (1 g, 0.08 mmol) was dissolved in anhydrous tetrahydrofuran (THF; 5 mL). 6-maleimidohexanoic acid (MA; 66 mg, 0.3 mmol) was dissolved in THF (5 ml), followed by the addition of 1.5 molar equivalents of dicyclohexylcarbodiimide (DCC, 98 mg, 0.5 mmol)

and 4-dimethylaminopyridine (DMAP, 57 mg, 0.5 mmol). Pluronic F127 was dissolved in THF with vigorous stirring and subsequently mixed slowly with the activated MA. The reaction mixture was then gently stirred for 24 h at room temperature, precipitated in diethyl ether, and dried under vacuum. Successful conjugation of MA with F127 was confirmed using ^{1}H-NMR (Figure S5). ^{1}H-NMR spectra were recorded in DMSO-d6 at room temperature using a Bruker NMR Spectrometer (Bruker, Germany) at 500 MHz.

^{1}H-NMR (500 MHz, DMSO-d_6) for MA-F127 conjugate (Figure S5): δ = 7.0 ppm (1H, s, −CH═C<u>H</u>-C═O of MA), 3.4–3.6 ppm (848H, m, −C<u>H</u>$_2$C<u>H</u>$_2$O– of pluronic F127), and 1.0 ppm (210H, d, −CH$_2$CH–(C<u>H</u>$_3$)O– of pluronic F127).

Preparation of the pH-Sensitive Pt-NA. MA–F127 (10 mg) and Pt nanoclusters (1.2 mg) were dissolved in $CHCl_3$ (3 mL). Octadecylamine–p(API-Asp)10 (20 mg) was dissolved in methanol (0.2 mL) and subsequently dropped into the MA-F127–Pt nanoclusters mixture with vigorous stirring. The final mixture was dried onto a film placed on the wall of a 25-mL round-bottom flask at 60°C under reduced pressure; 4 mL of phosphate-buffered saline (PBS; pH 7.4) was then added to the flask to hydrate the formed film. After ultrasonication for 5 min with a probe sonicator (Sonics Vibra cell, Sonics & Material, Inc., New Town, CT, USA), the solution was stirred continuously at 60°C for 6 h. The Pt-NA were purified by centrifugation at 15,000 rpm (4 C°, 15 min) and washed three times with PBS buffer (150 mM, pH 7.4) to remove unreacted MA-F127 or other reagents.

Incorporation of SP94 Peptide onto pH-Sensitive Pt-NA. SP94 peptide was incorporated onto to the pH-sensitive Pt-NA by the reaction between maleimide group of MA-F127 and thiol group (–SH) of SP94 peptide.[3] The SP94 was then reacted with pH-sensitive pt-NP assembles at a peptide-to-MA-F127 molar ratio of 1:10 for 3 h at room temperature in PBS

(pH=7.4). Unreacted SP94 was removed by a centrifugal filter (molecular weight cut-off: 100 kDa, Pall life sciences, Port Washington, NY, USA).

Preparation of pH-Insensitive Pt Nanocluster Assembles. The pH-insensitive Pt Nanocluster assembles (InS-Pt) was prepared by following the protocol for pH-sensitive Pt-NA as described above. However, the pH-sensitive peptide ligand (octadecylamine-p(API-Asp)$_{10}$) was replaced with pH-insensitive peptide ligand (octadecylamine-PBLA$_{10}$) in the preparation process.

Preparation of Fluorescence-Labeled Pt-NA and InS-Pt. The fluorescence- labeled Pt-NA and InS-Pt were prepared by following the protocol for Pt-NA and InS-Pt as described above. However, the peptide ligands (octadecylamine-p(API-Asp)$_{10}$ or octadecylamine-PBLA$_{10}$) were replaced with fluorescence-labeled peptide ligands in the preparation process.

Measurement of Proton Buffering Capacity of Pt-NA. The proton buffering capacity of Pt-NA was measured by an acid–base titration method. In brief, Pt-NA (30 mg) was dissolved in 150 mm NaCl (5 ml), and the solution was adjusted to pH 10 by adding 1 N NaOH. The polymer solution was titrated with 0.01 N HCl, and its pH was monitored by disital pH meter (Mettler-Toledo, Schwerzenbach, Switzerland).

Transmittance Measurement of Pt-NA at Different pH. The light transmittance measurements of Pt-NA solutions (5 mg ml^{-1}) were obtained using a UV–Visible spectrophotometer (UV-2450; Shimadzu, Japan) at 500 nm while the pH value of solution was gradually decreased from 10 to 3 by adding 0.1 N HCl.

Particle Size Measurement of Pt-NA at Different pH. The particle size of Pt-NA (1 mg ml^{-1}) was determined at different pH by dynamic light scattering (DLS, Zetasizer Nano ZS, Malvern Instruments Ltd., UK).

Measurement of Released Pt Ions from Pt-NA at Different pH. The Pt ion release experiments were conducted using dialysis tubes (Float-A-Lyzer®; cutoff 0.1-0.5 kDa, Spectrum® Laboratories, Inc., USA) at 37 °C. Typically, Pt-NA (Pt, 20 μg mL^{-1}) in 1 mL deionized water were placed in a dialysis tube and dialyzed against 10 mL of PBS (pH 7.4, 6.0, and 5.0) with shaking at 200 rpm. At hourly intervals, the release medium (10 mL) was taken out and the same volume of fresh PBS was added to the release medium. The amount of released Pt was quantified using inductively coupled plasma mass spectrometry (ICP-MS, Perkin Elmer, Waltham, MA, USA).

Establishment of cisplatin-resistant human liver cancer cell lines. The HuH7 cells were bought from Japanese Collection of Research Bioresources (JCRB) Cell Bank (Osaka, Japan) and the PLC/PRF/5 cells were bought from American Type Culture Collection (ATCC) (Manassas, VA). The cells were cultured in Dulbecco's modified Eagle's medium (DMEM) with 10% FBS and 100 units mL^{-1} of penicillin and 100 μg mL^{-1} of streptomycin (Invitrogen, Carlsbad, CA) at 37°C in the presence of 5% CO_2. The cells were treated with gradually increasing concentrations of cisplatin (starting from 1ug mL^{-1}).When the treated cells entered the logarithmic growth phase, the concentration of cisplatin was increased. Finally, the cells that could proliferate in the presence of 10 ug ml^{-1} cisplatin were obtained and designated as HuH7-Cis and PLC/PRF/5-Cis cells.[4,5]

Cell Viability Assay. The cell viability was assessed by 3-(4,5-dimethylthiazol-2-yl)-5-(3-carboxymethoxyphenyl)-2-(4-sulphophenyl)-2H-tetrazolium (MTS) assays using the CellTiter 96 AQueous One Solution Cell Proliferation Assay kit (Promega) following the manufacturer's instructions. The cells were seeded in a 96-well plate at a density of ~5×10^3 cells per well. Following one day after seeding, the culture medium was replaced with fresh DMEM containing Pt-NA, cisplatin or vehicle control at indicated concentration and incubated for 48 hours. Each experiment was repeated three times.

Flow cytometry analysis. Flow cytometry was performed in the SingHealth Flow Cytometry Core Platform. The isolated cells in culture were treated with Pt-NA, cisplatin or vehicle control for 48 h and detached by Trypsin-EDTA (0.25%) treatment. The cells were collected and fixed with 70% ethanol for 30 min at 4°C and permeabilized with 100 ug ml^{-1} digitonin in PBS. The sample was incubated with the Anti-Cisplatin modified DNA antibody [CP9/19] (ab103261) (1/200 in PBS + 1% FBS) for 18 h at 4°C. A FITC-conjugated rabbit anti-rat IgG H&L polyclonal (1/200) was used as the secondary antibody (Abcam, Cambridge, MA, USA). The samples were analyzed on a BD FACSAria (BD Biosciences) for FITC positive cells.

Immunofluorescence staining. The isolated cells were plated onto coverslips and placed in a six well plate. In the next day, the cells were treated with Pt-NA, cisplatin or vehicle control for 48 h, fixed with 4% formaldehyde, permeabilized with 0.5% Triton X-100 and blocked with 0.5% BSA and 0.3% Triton-X-100 in PBS. Thereafter, the cells were incubated with primary antibody anti-cisplatin (CP9/19) (Abcam, Cambridge, MA, USA) that was diluted 1: 500 for 18 h at 4°C. Secondary antibodies labeled with FITC (Sigma-Aldrich) were added at 1 : 1000 and incubated at room temperature for 2 h. Slides were mounted with a

mounting-solution reagent containing Hoechst 33342 ((Molecular Probes, Life Technologies Carlsbad, CA, USA)) and then analyzed using a Nikon fluorescence microscope.

Flow Cytometry Analysis and Fluorescence-Activated Cell Sorting (FACS). Flow cytometry was performed in the SingHealth Flow Cytometry Core Platform. For isolation of the SP and CD24+ cell population, the cells were stained with Vybrant® DyeCycle™ Violet Stain (Catalogue no. V35003, Invitrogen) and fluorescein isothiocyanate-conjugated CD24 antibody (BD Biosciences), or with isotype-matched mouse immunoglobulin as a control. Samples were analysed and sorted on a BD FACSAria (BD Biosciences) flow cytometer. The cells were detached from the dishes with Trypsin-EDTA (Invitrogen) and resuspended at a density of 1×10^6 cells ml^{-1} in the DMEM with 10% heat-inactivated fetal bovine serum (FBS) and 10 mM HEPES. The verapamil was added with the concentration of 400 μM for treatment of 30 min. These cells were then incubated at 37 °C for 30 min with the final stain concentration of 5 μM Vybrant® DyeCycle™ Violet Stain (Catalog no. V35003, Invitrogen). The samples were analyzed and sorted without washing or fixing on the BD FACSAria (BD Biosciences) using ~405 nm excitation and ~440 nm emission. We washed the cells twice and resuspended in 2% FBS-phosphate-buffered saline (PBS). For the analysis or isolation of CD24+ cell populations, cells were then incubated with CD24-fluorescein isothiocyanate (FITC) or isotype-matched mouse immunoglobulin as a control (BD Pharmingen, San Diego, CA) for 30 min. The samples were washed twice and analyzed or sorted on a BD FACSAria (BD Biosciences).

Cellular Uptake Assay. The sorted SP+CD24+ HCCLM3 cells or MIHA cells were seeded in an 8-well cover-glass chamber (LAB-TEK, Nagle Nunc, IL, USA) overnight. The Pt-NA medium was then added at different concentrations and the cells were incubated for 24 hours.

Cellular uptake of the Pt-NA was observed using a Nikon live-cell imaging system (Nikon). The cellular uptake behaviour and intracellular distribution of the Pt-NA were also analysed using CLSM (Carl Zeiss). The nucleus was counterstained by the Hoechst 33342. For the *in vivo* uptake assay, once the orthotopic xenograft tumors were established from the sorted SP+CD24+ luciferase-expressing HCCLM3 cells, the mice were imaged using the Xenogen IVIS Lumina system after tail vein injection of the Pt-NA.

Confocal Imaging of Uptake and Endosome Escape of Pt-NA in SP+CD24+ HCCLM3 Cells. The cells were cultured in glass bottom dishes (MatTek, MA) and transfected with CellLight® Late Endosomes-GFP, BacMam 2.0 (Molecular Probes, OR) for Rab7a (endosome marker) labeling. Cells were then cultured in growth medium for Pt-NA treatment at concentration of 1ug mL^{-1} at pH 7.4. Confocal images were captured at 1 h and 4 h after treatment by Nikon N-STORM super-resolution confocal microscope with a 100× objective lens. The images were analyzed by Nikon Software NIS-Elements.

Measurement of Pt by Inductively Coupled Plasma Mass Spectrometry (ICP-MS) Uptake of Pt was determined by ICP-MS. The cells were treated by cisplatin or Pt-NA and then digested overnight in 3 ml HNO_3 and 1 ml H_2O_2. On the next day, 1 ml of aqua regia was added, and then the sample was allowed to react for another 1-2 hrs. The sample solution was then diluted to 100 mL with de-ionized water, and aqua regia (final concentration: 5%). Then the sample solution was measured by ICP-MS on a Perkin Elmer Elan 6100. A series of Pt solutions were prepared before each experiment. The resulting calibration line was used to determine the amount of Pt in each fraction.

DNA Damage Assay. The sorted SP+CD24+ HCCLM3 and PLC/PRF/5-Cis cells were seeded in the BD Falcon™ 8-well CultureSlide and treated with the Pt-NA or cisplatin for 48 h.

The treated cells were fixed and incubated with primary antibodies against γ-H2AX and then further incubated with the secondary antibody Alexa Fluor® 488 goat anti-rabbit IgG (Invitrogen). Slides were counterstained with Hoechst 33342 and were imaged using the Zeiss LSM510 CLSM Imaging System.

Sphere Formation Assay. The sorted SP+CD24+ HCCLM3 and PLC/PRF/5-Cis cells (2×10^3) were plated onto a 6-well ultra-low attachment plate (Corning, Corning, NY) in serum-free DMEM-F12, supplemented with 2 mM L-glutamine, 1% sodium pyruvate (Invitrogen), 1% MEM nonessential amino acids (Invitrogen), 1% insulin-transferrin-selenium-X supplement (Invitrogen), 1 μM dexamethasone (Wako), 200 μM L-ascorbic acid 2-phosphate (Sigma-Aldrich), 10 mM nicotinamide (Wako), 100 μg ml^{-1} penicillin, and 100 U ml^{-1} streptomycin supplemented with 20 ng ml^{-1} epithelial growth factor and 10 ng ml^{-1} fibroblast growth factor-2 (Invitrogen). After 2-3 weeks of culture, the number of tumorspheres (diameter > 40 μm) was manually counted in three randomly selected fields at the magnification of 40X using an inverted fluorescence microscope. Results were obtained from three independent experiments performed in triplicate.

***In vivo* Tumorigenicity and Treatment Assay.** All experiments using mice were approved by the SingHealth Institutional Animal Care and Use Committee (IACUC). Different numbers of sorted SP−CD24− or SP+CD24+ HCCLM3 and PLC/PRF/5-Cis cells were injected subcutaneously into the NOD/SCID mice. The subcutaneous tumors were collected, and similar-sized tumors were transplanted into the livers of mice to establish the orthotopic xenograft model. Once the orthotopic xenograft tumors were established from sorted SP+CD24+ luciferase-expressing HCCLM3 cells, the mice with similar bioluminescence-imaging signals were divided into groups (6 mice per group) and

administered cisplatin (2 mg kg^{-1}), Pt-NA (2 mg kg^{-1}), sorafenib (20 mg kg^{-1}) or vehicle control intravenously by tail vein injection or orally (for sorafenib). The sorafenib was administered every day, whereas the other drugs were administered twice per week. The therapeutic efficacy was determined according to mouse survival and tumor size was estimated by bioluminescence imaging from the Xenogen IVIS Lumina system following luciferin administration. In addition, to compare with cisplatin-incorporating polymeric micelles (cisplatin loaded poly (L-glutamic acid)-g-methoxy poly (ethylene glycol) complex nanoparticles, Nanoplatin), the mice models were established and divided into two groups (5 mice per group) and administered or Pt-NA (2 mg kg^{-1}) intravenously by tail vein injection twice per week. The therapeutic efficacy was determined according to the tumor size estimated by bioluminescence imaging from the Xenogen IVIS Lumina system following luciferin administration.

Tissue Specimens and Cell Culture. The collection of tumor and adjacent normal liver tissues from HCC patients was approved by our Institutional Review Board (IRB) and all tissues studied were provided by the Tissue Repository of the National Cancer Centre Singapore (NCCS). Written informed consent was obtained from all participating patients and all clinical and histopathological data provided to the researchers were rendered anonymous. All cells were purchased from the American Type Culture Collection (ATCC), Korean Cell Line Bank (KCLB), and Japanese Collection of Research Bioresources (JCRB) cell bank and cultured according to standard protocols of ATCC, KCLB and JCRB. Cells were grown at 37°C in a 5% CO_2 humidified atmosphere. Liver cancer cells were cultured in Dulbecco's modified Eagle's medium (DMEM for HepG2, HuH7, PLC/PRF/5, HCCLM3, HLE, Mahlavu, SNU-449, SK-HEP-1, JHH-4, HuH1), or William's E medium (for JHH-1, JHH-2, JHH-5 and JHH-7), or RPMI 1640 medium (for SNU-354, SNU-368, SNU-387, SNU-398, SNU-423,

SNU-739, SNU-761, SNU-878 and SNU-886) with 10% FBS and 100 units mL^{-1} of penicillin and 100 μg mL^{-1} of streptomycin (Invitrogen, Carlsbad, CA). All cell lines were maintained at 37 °C in the presence of 5% CO_2. Sorafenib was from Bayer HealthCare Pharmaceuticals, Inc.

Microarray and Real-Time Quantitative RT-PCR (qRT-PCR) Analysis. Our group has previously established a global gene profile database on HCC tumor tissues and histologically normal liver tissues using Affymetrix Human Genome U133 plus 2.0 Arrays (Affymetrix, Santa Clara, CA, USA)[6,7]. For the gene expression profile analysis on sorted SP+CD24+ HCCLM3 cells treated with Pt-NA or vehicle control. Total RNA was extracted using TRIzol reagent (Invitrogen). The quality and quantity of isolated total RNA were assessed using the Agilent 2100 Bioanalyzer and NanoDrop ND-1000 Spectrophotometer (Agilent, Santa Clara, CA, USA). Microarray analysis was performed as we described using the GeneChip® Human Gene ST2.0 Arrays (Affymetrix, USA) according to the manufacturers' instructions. For mRNA detection by qRT-PCR, the total RNA was reversely transcribed using SuperScript III First-Strand Synthesis System for RT-PCR (Invitrogen, CA). qPCR was performed using SsoFast™ EvaGreen® Supermix (Bio-Rad) with hypoxanthine phosphoribosyltransferase 1 (HPRT1) as an internal control, and concentration differences were calculated via relative quantification (2-ΔCt). The survival curves were created using the Kaplan-Meier method and statistically compared using a log-rank test.

Immunohistochemistry (IHC). The paraffin-embedded tissue samples from consenting patients were cut in 5-μm sections and placed on polylysine coated slides, deparaffinized in xylene and rehydrated using a series of graded alcohols. Antigen retrieval was performed by heat mediation in citrate buffer (pH 6) (Dako). Samples were blocked with 10% goat serum before incubating with primary antibody. The samples were incubated overnight using a

primary antibody; anti-CD24, *ABCG2*, *CCNB1*, *CDK1* and *TOP2A* (1:100) (Abcam) or an isotype-matched IgG as a negative control in a humidified container at 4 °C. Immunohistochemical staining was performed with the Dako Envision Plus System (Dako, Carpinteria, CA) according to the manufacturer's instructions. The intensity of staining was evaluated on the scale of 0 to 4 according to the percentage of positive tumors.

Survival and Statistical Analysis. The experimental data are presented as the mean ± standard deviation. The survival curves were derived using the Kaplan-Meier method and were statistically compared using a log-rank test. Other statistical comparisons were performed using analysis of variance or a two-tailed Student's t-test in GraphPad Prism 5 software. Differences were considered statistically significant when the P-values were less than 0.05.

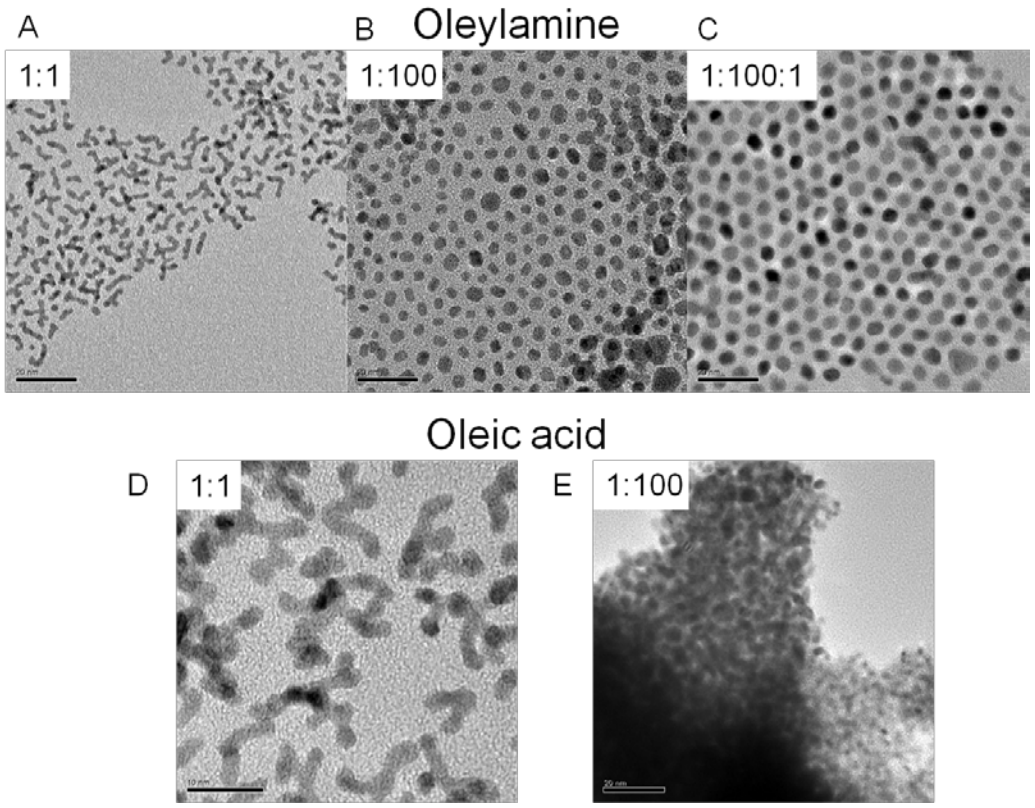

Figure S1. TEM images of Pt nanocrystals synthesized in different conditions. (A) $Pt(acac)_2$: oleylamine=1:1. (B) $Pt(acac)_2$: oleylamine=1:100. (C) $Pt(acac)_2$: oleylamine: oleic acid=1:100:1. (D) $Pt(acac)_2$: oleic acid=1:1. (E) $Pt(acac)_2$: oleic acid=1:100.

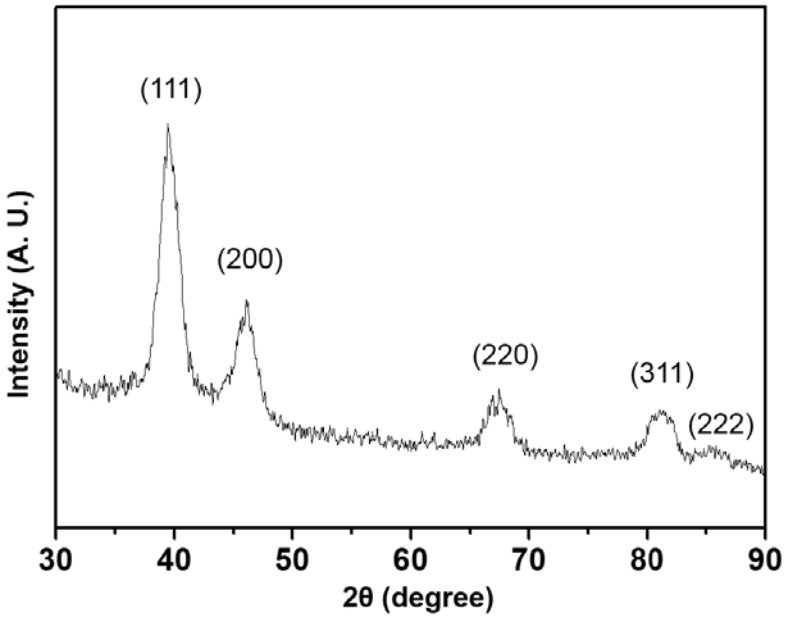

Figure S2. XRD pattern of synthesized Pt nanocrystals.

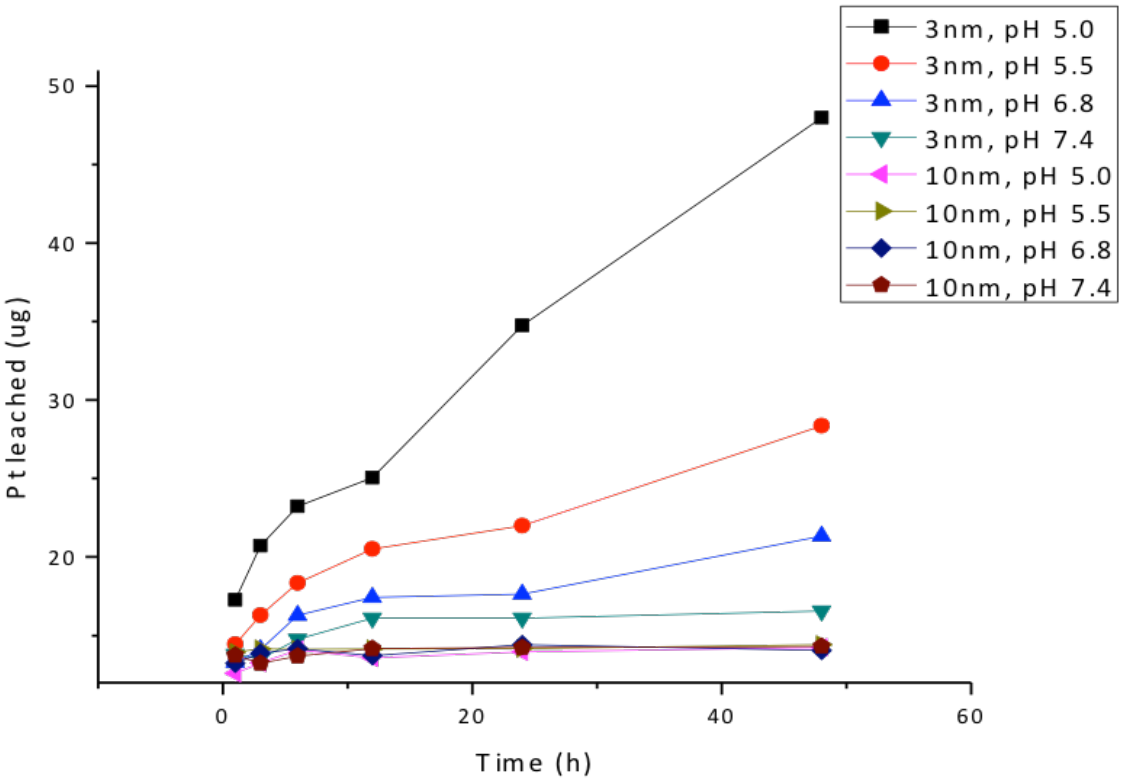

Figure S3. *In vitro* cumulative Pt ions release from Pt nanocrystals with particle size 3 nm and 10 nm at different pH (pH 7.4, 6.8, 5.5 and 5.0, Pt sample 5mg ml^{-1}).

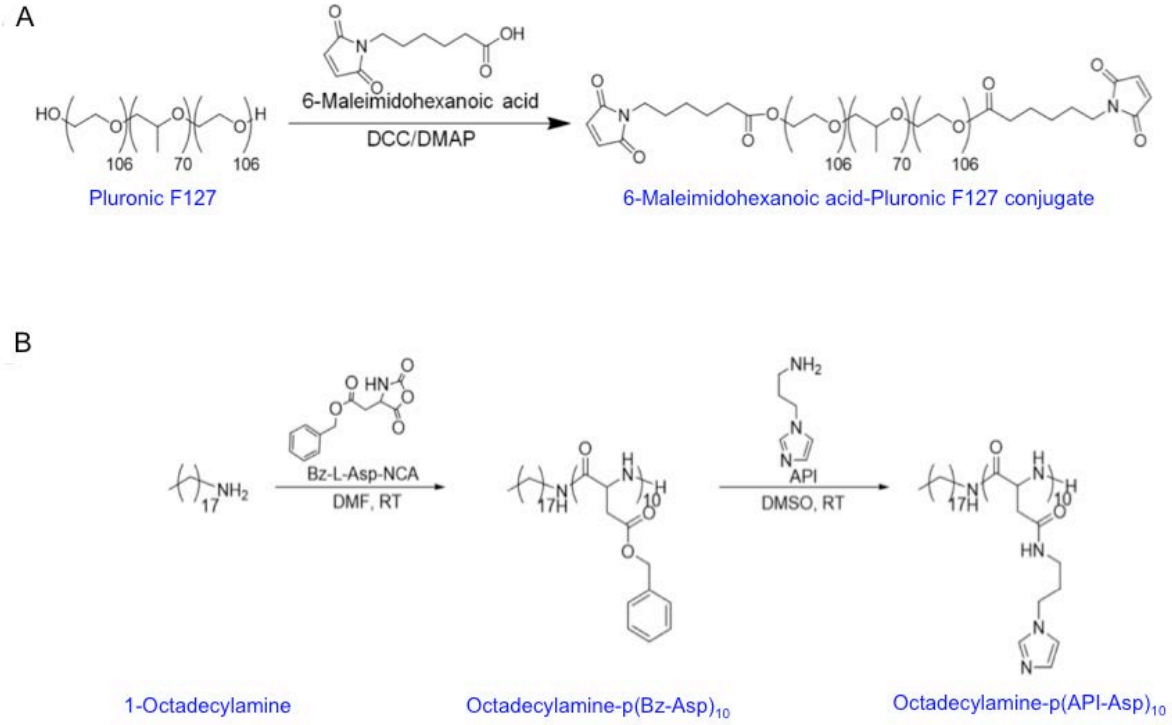

Figure S4. Synthetic scheme of two polymeric ligands for Pt nanocluster assembly. (A) Synthesis of 6-aleimidohexanoic acid-pluronic F127 (MA-F127) conjugates. (B) Synthesis of pH-sensitive polypeptide (octadecylamine-p(API-Asp)$_{10}$).

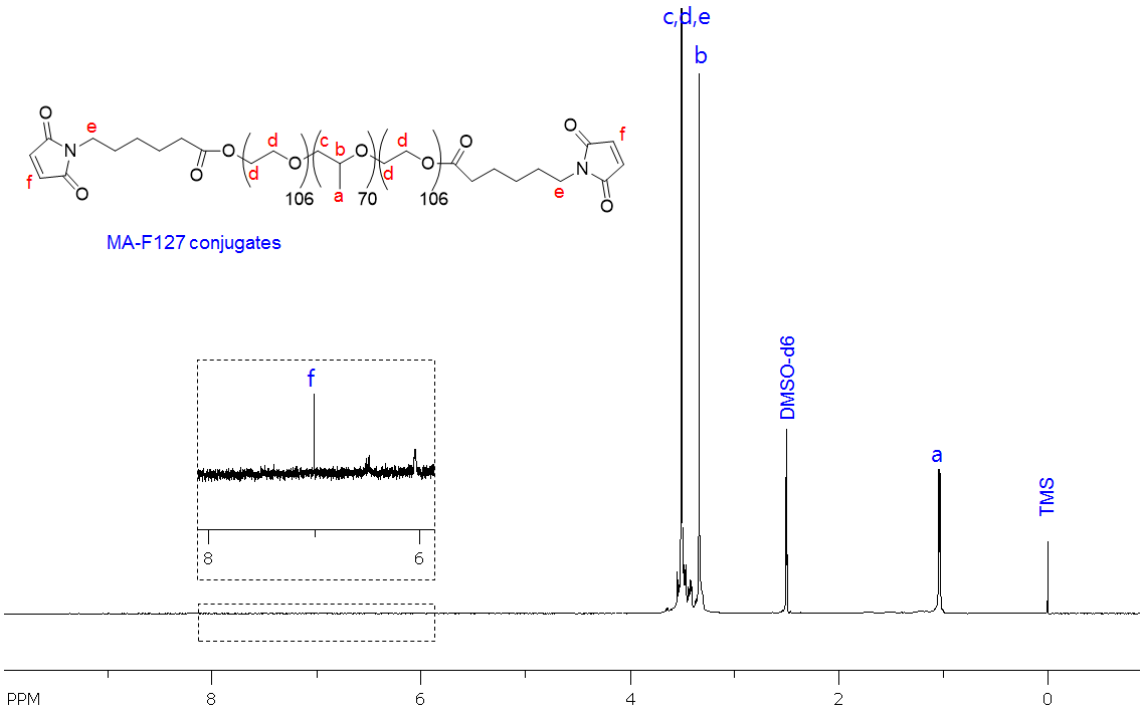

Figure S5. ^{1}H-NMR spectrum of MA-F127 conjugates in DMSO-d_6.

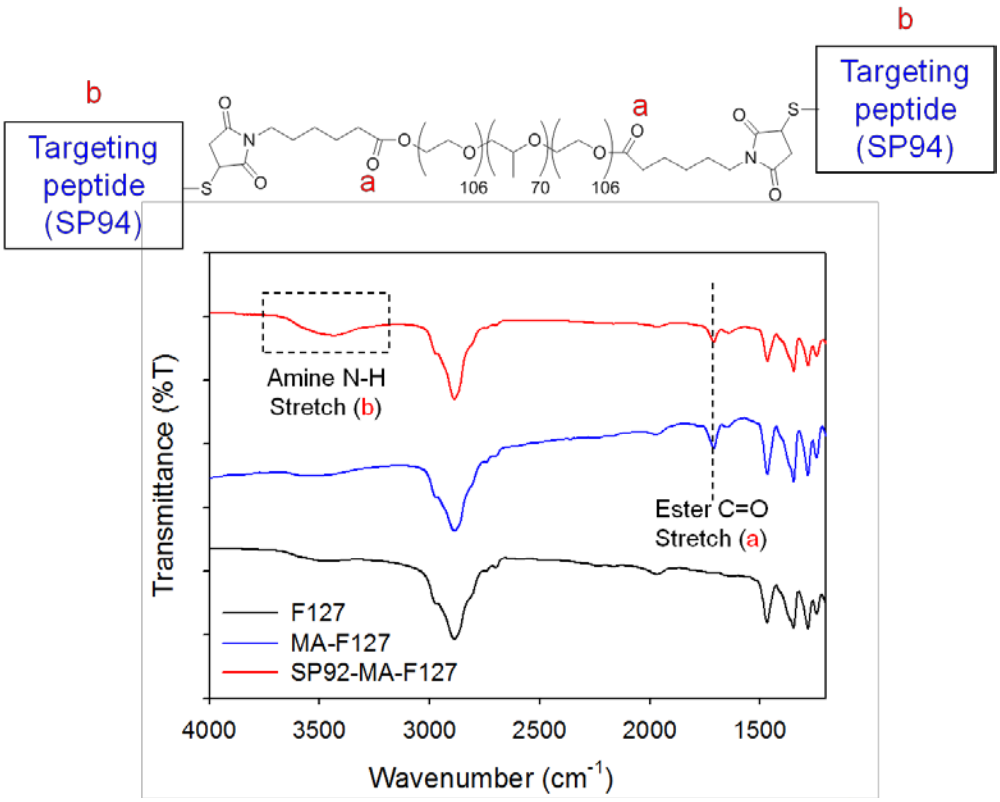

Figure S6. The successful conjugation of targeting peptide (SP94) with pH-sensitive Pt-NA was confirmed by Fourier transform infrared (FT-IR) spectroscopy. After addition of SP94, the characteristic bands of amine N-H stretch of peptide appeared at 3500-3300 cm^{-1}.

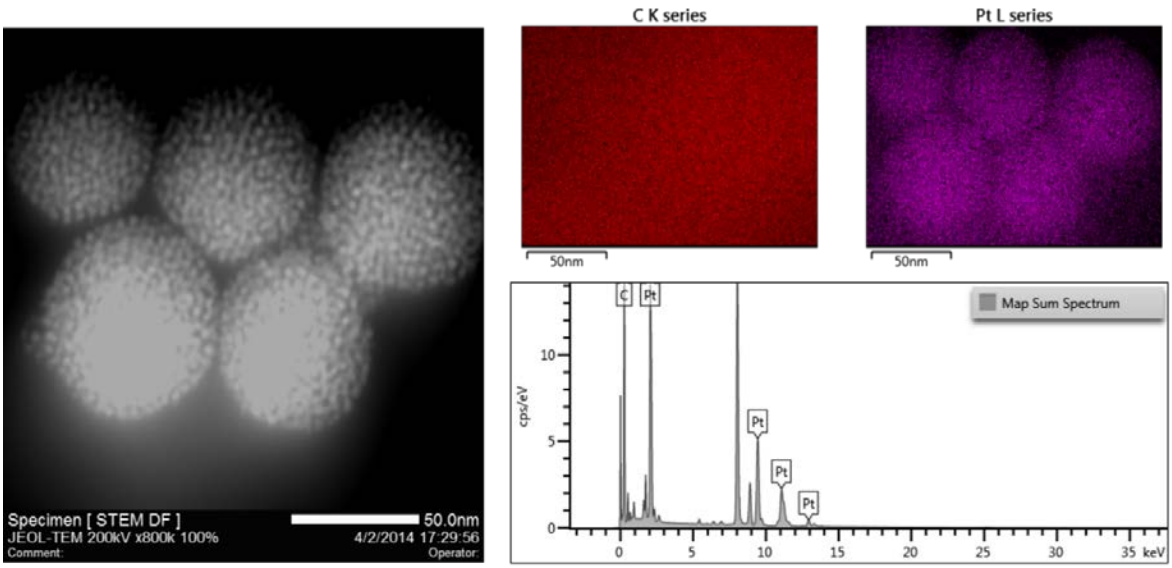

Figure S7. STEM and EELS analysis of Pt-NA.

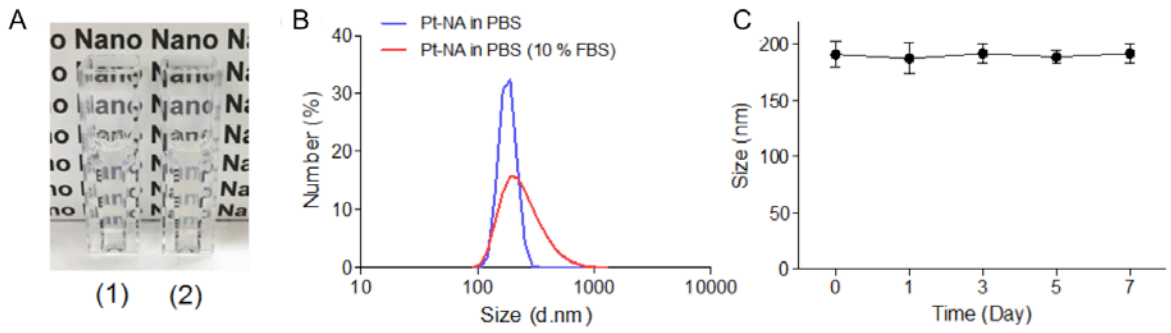

Figure S8. Stability of Pt-NA in serum condition. (A) Digital photographs of Pt-NA suspension in (1) PBS or (2) 10% FBS/PBS solution. (B) Size distribution of Pt-NA in PBS or 10% FBS/PBS solution (concentration of Pt-NA: 1 mg mL^{-1}). (C) Time-dependent stability of Pt-NA in 10% FBS/PBS solution at room temperature. Although the particle size of Pt-NA increases slightly in 10% FBS/PBS solution, no agglomeration is observed in both PBS and 10% FBS/PBS solution. In addition, the particle size of Pt-NA remains stable for a week in 10% FBS/PBS solution.

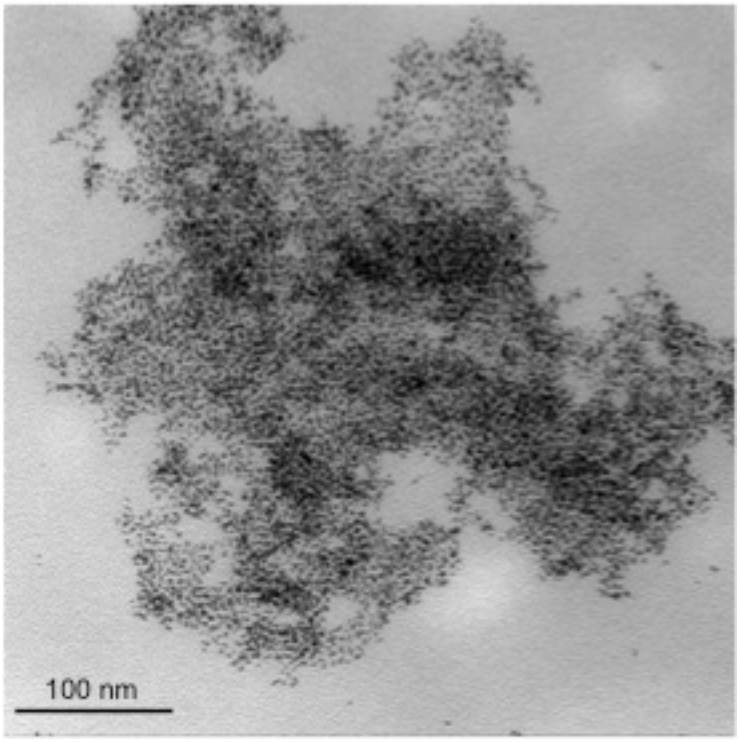

Figure S9. TEM image of Pt assembly dissociation at pH 6.0. (scale bar: 100 nm)

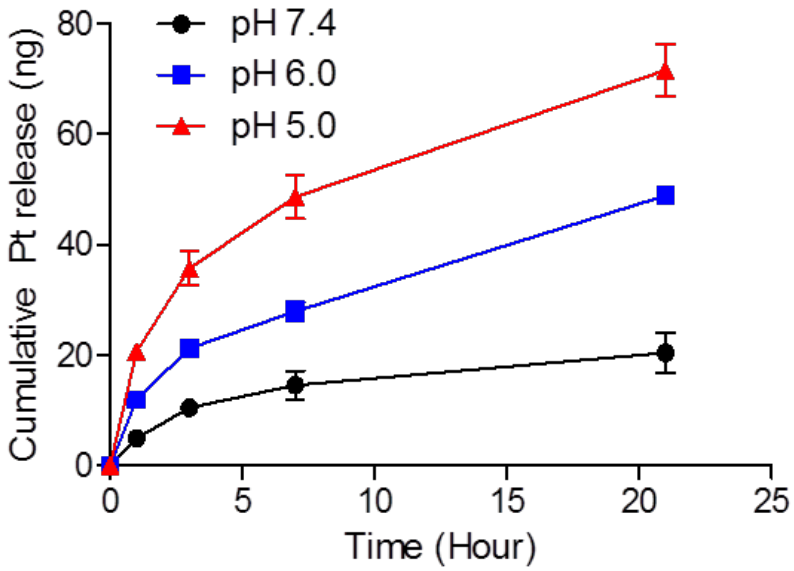

Figure S10. *In vitro* cumulative Pt ions release from Pt-NA at different pH (pH 7.4, 6.0 and 5.0, Pt sample 20 μg ml^{-1}).

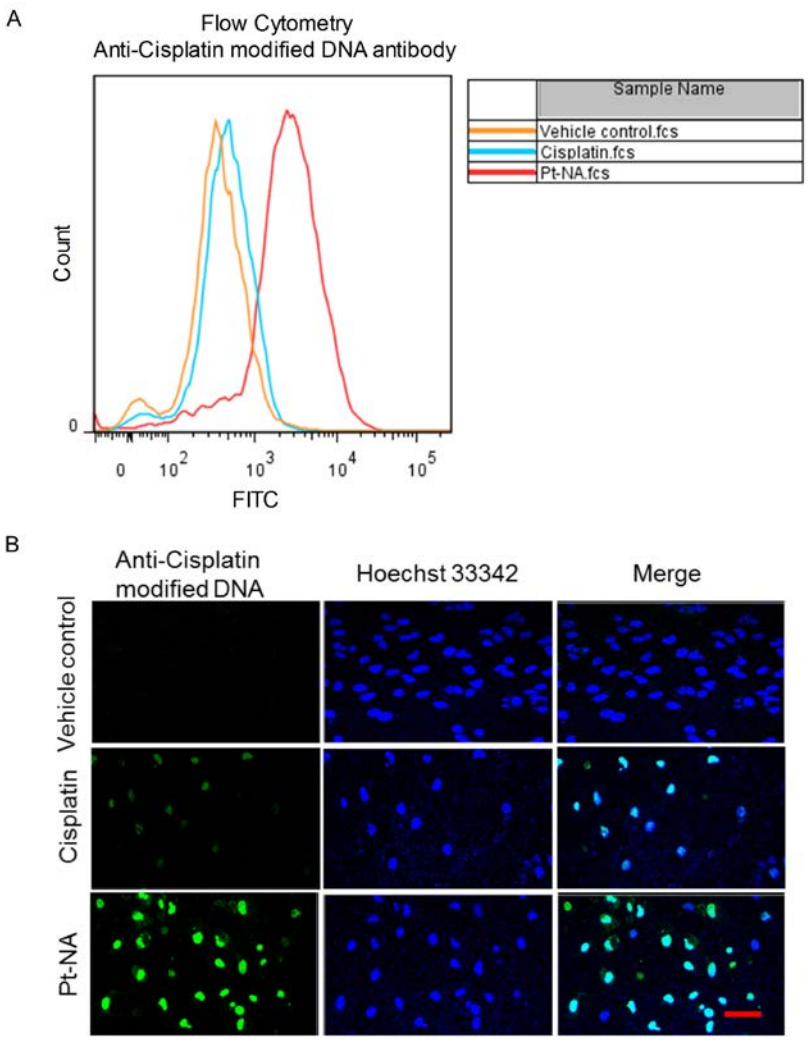

Figures S11. The quantification of Pt-NA-induced adducts on DNA. (A) The representative flow cytometry analysis images showed that significant positive staining with anti-cisplatin adduct antibody upon Pt-NA treatment, whereas the vehicle control or cisplatin treated cells did not show or weak positive staining with anti-cisplatin adduct antibody. (B) The representative immunofluorescence images showed that there was a significant increase of Pt-DNA adducts in Pt-NA treatment cells, but no vehicle control or cisplatin treated cells as detected with anti-Pt adduct antibody.

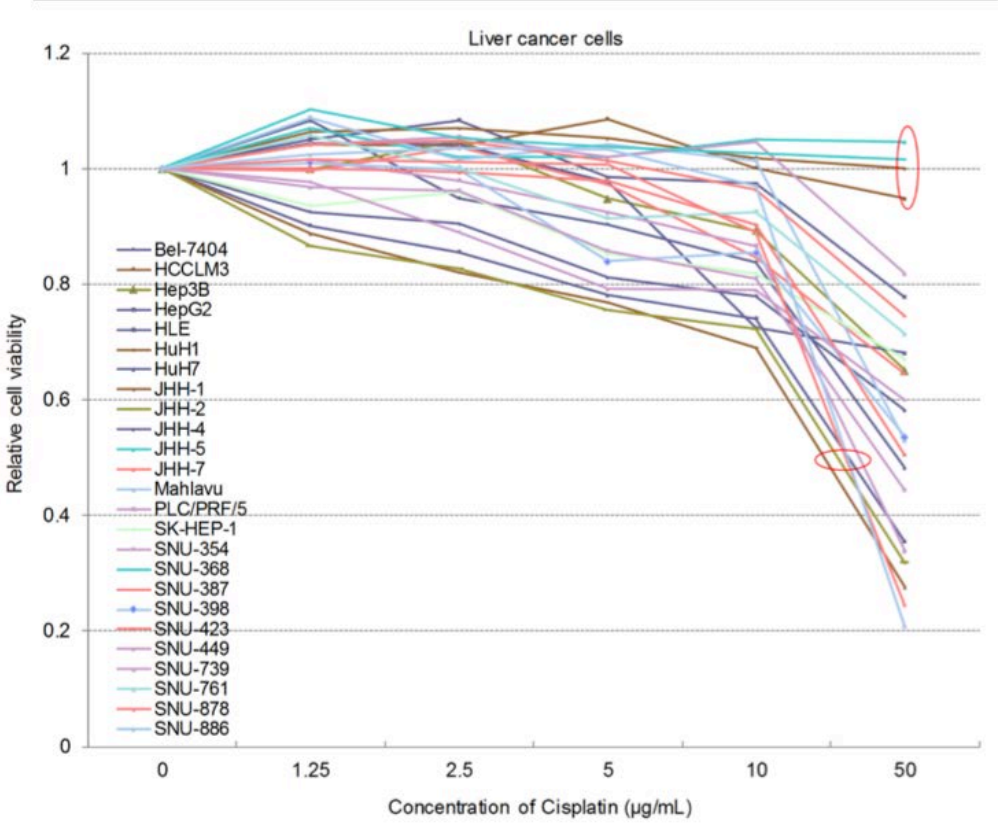

Figure S12. The heterogeneity sensitivity of liver cancer cells to cisplatin *in vitro*.

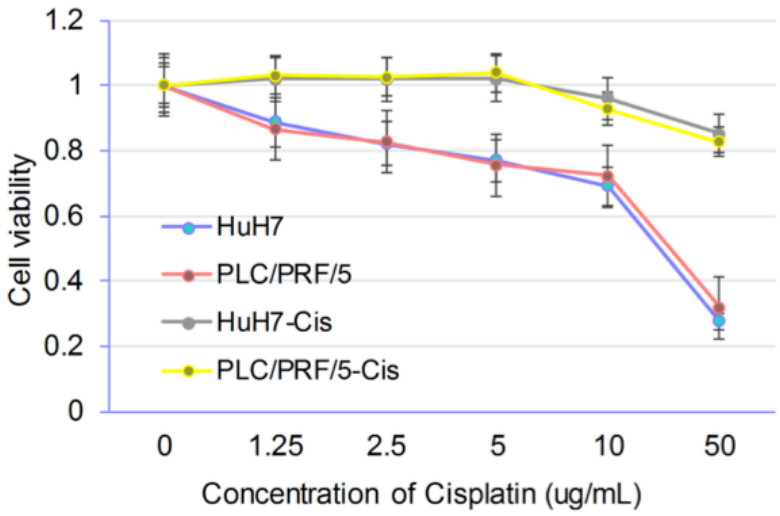

Figure S13. The relative cisplatin sensitive HuH7 and PLC/PRF/5 cells were induced to cisplatin resistance (HuH7-Cis and PLC/PRF/5-Cis) with increased dose of cisplatin treatment for six months.

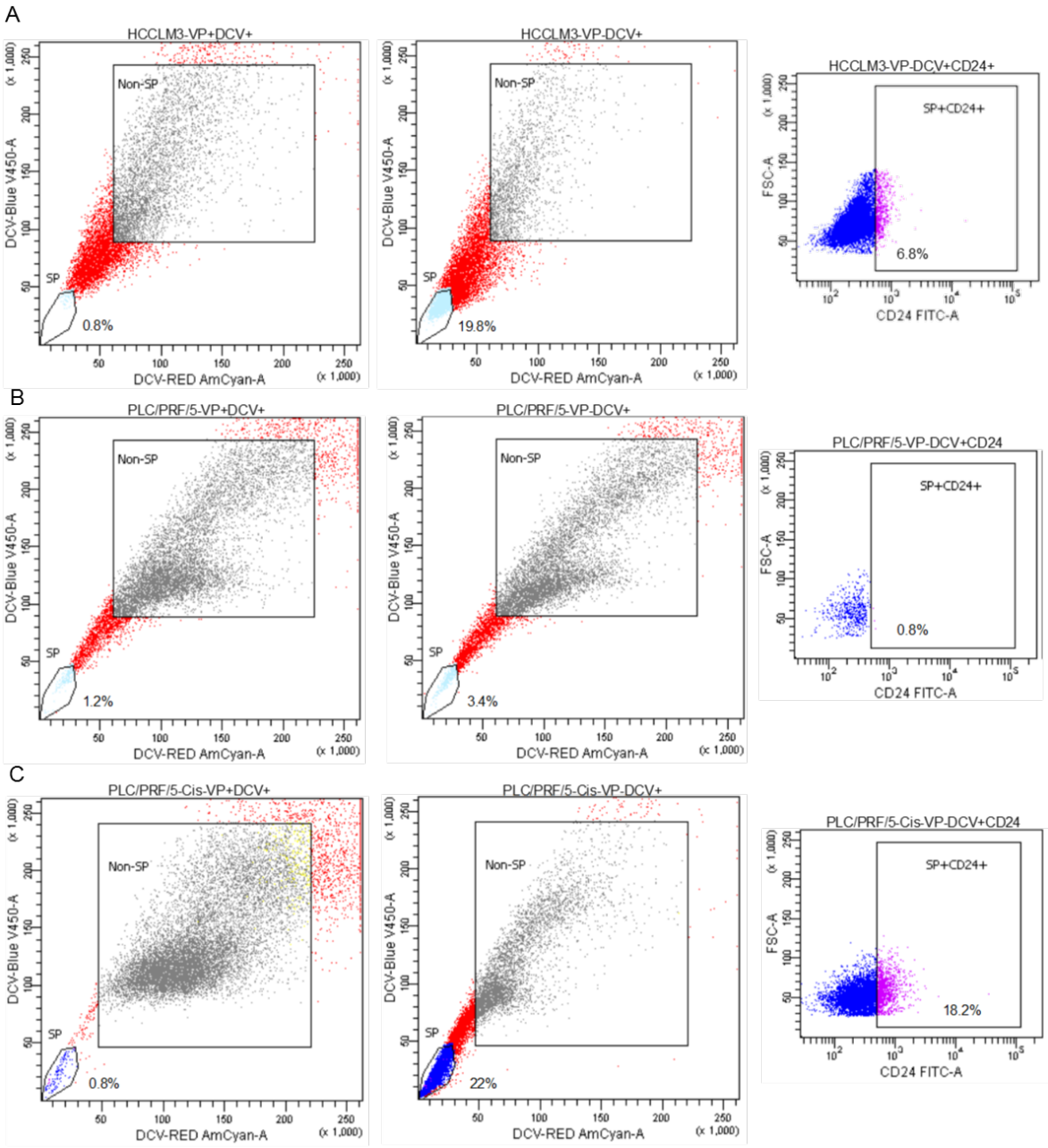

Figure S14. Representative images and percentage of SP and SP+CD24+ cells: (A) in cisplatin-resistant HCCLM3 cell line. (B) in the cisplatin-sensitive cell line PLC/PRF/5. (C) in PLC/PRF/5-Cis cells with induced cisplatin resistance. Rightmost representative images represent the percentage of sequentially sorted CD24+ cells from the first sorted SP+ cells in the middle column.

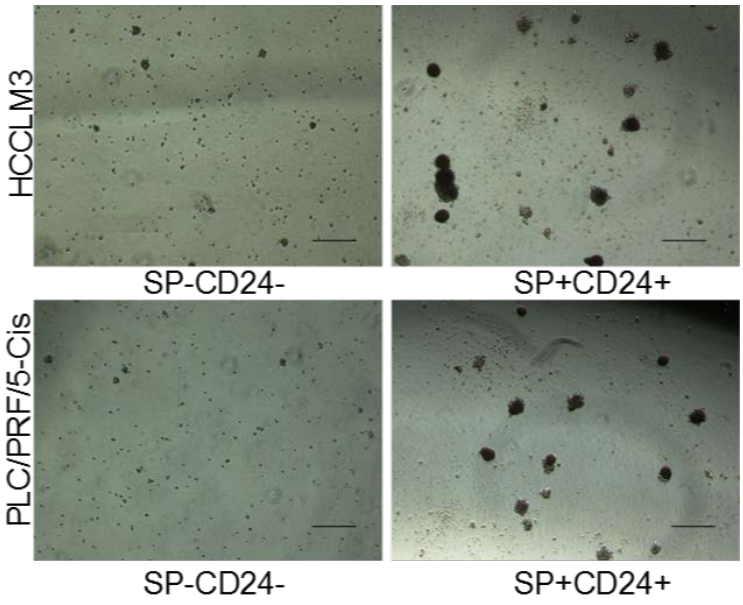

Figure S15. Sphere-forming assay results show that the *in vitro* self-renewal ability was enhanced in SP+CD24+ cells from cisplatin-resistant HCCLM3 and PLC/PRF/5-Cis cells (scale bar=100μM). The higher self-renewal ability of SP+CD24+ cells represents more drug resistance and regeneration probability of a tumor in the xenograft assay.

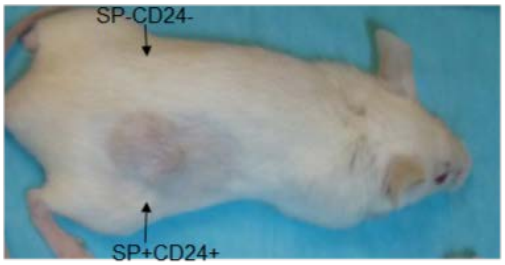

Tumor formation of sorted cells from HCCLM3				
	Tumors/Injection (60days)			
	10000	5000	1000	
SP-CD24-	2/5	1/5	0/5	3/15 (20%)
SP+CD24+	5/5	4/5	3/5	12/15 (80%)

Figure S16. The tumor-formation ability of sorted SP−CD24− and SP+CD24+ HCCLM3 cells. As few as 1,000 SP+CD24+ HCCLM3 cells induced tumor formation, whereas tumor formation is not induced from more than 10,000 sorted SP−CD24−cells. The right flanks were injected with SP+CD24+ cells and the left flanks were injected with SP−CD24− cells.

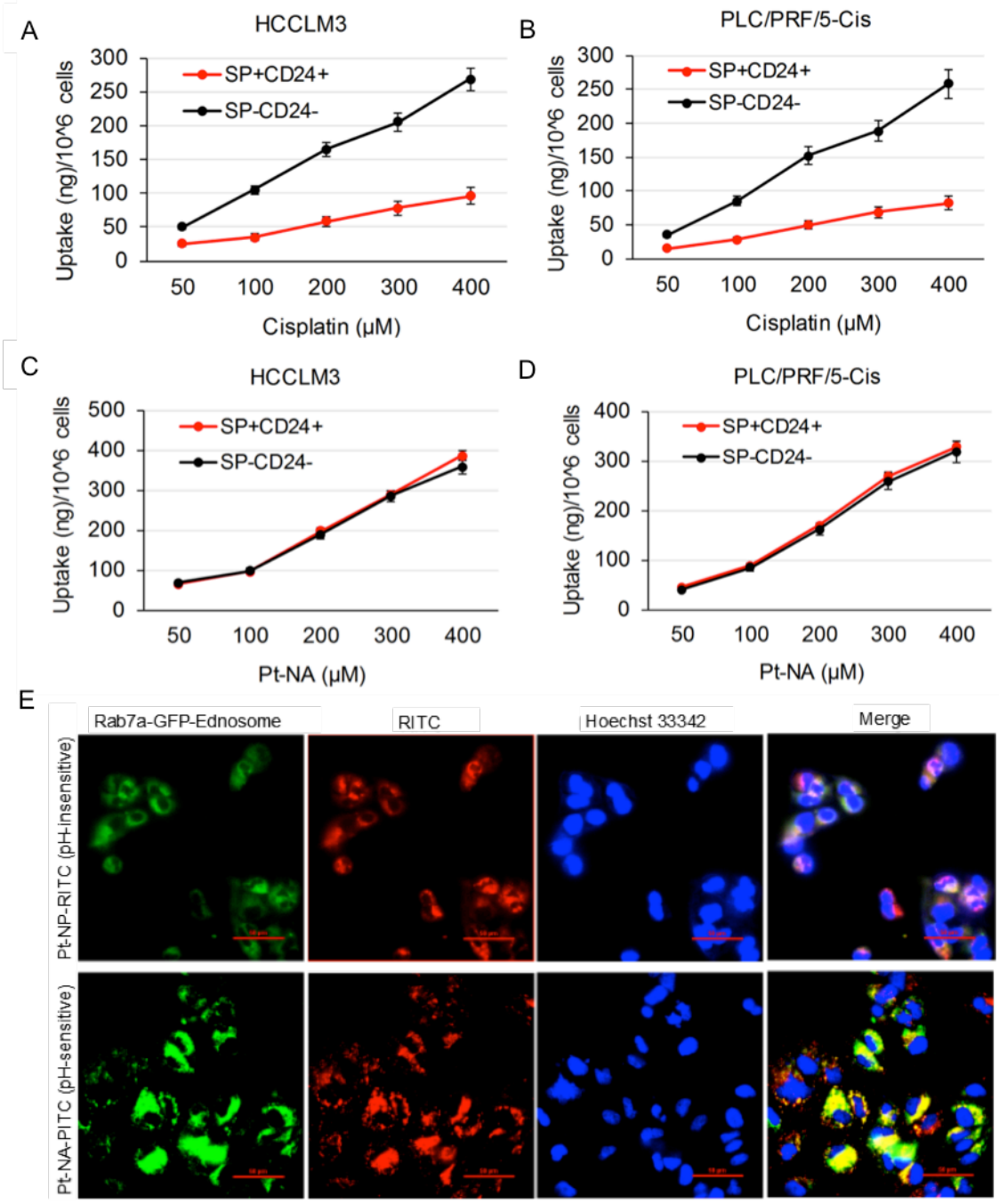

Figure S17. Pt uptake in SP−CD24− and SP+CD24+ cells from the HCCLM3 and PLC/PRF/5-Cis cells treated with cisplatin or Pt-NA. Cells were incubated for 3 h with media containing different concentrations of cisplatin or Pt-NA. (A), (B) Pt uptake in SP−CD24− and

SP+CD24+ cells from the HCCLM3 (A) and PLC/PRF/5-Cis (B) cells treated with cisplatin was measured using inductively coupled plasma mass spectrometry (ICP-MS). (C), (D) Pt uptake in SP−CD24− and SP+CD24+ cells from the HCCLM3 (C) and PLC/PRF/5-Cis (D) cells treated with Pt-NA. (E) Representative images showing the fluorescent signals of endosome marker (green) and Pt-NA-RITC (red) in SP+CD24+ HCCLM3 cells after incubation with pH sensitive Pt-NA or pH insensitive nanoparticles (Pt-NPs) control in serum-free medium for 4 hours. The endosome escape was shown in the cells incubation with pH sensitive Pt-NA. (Scale bar, 50 μm)

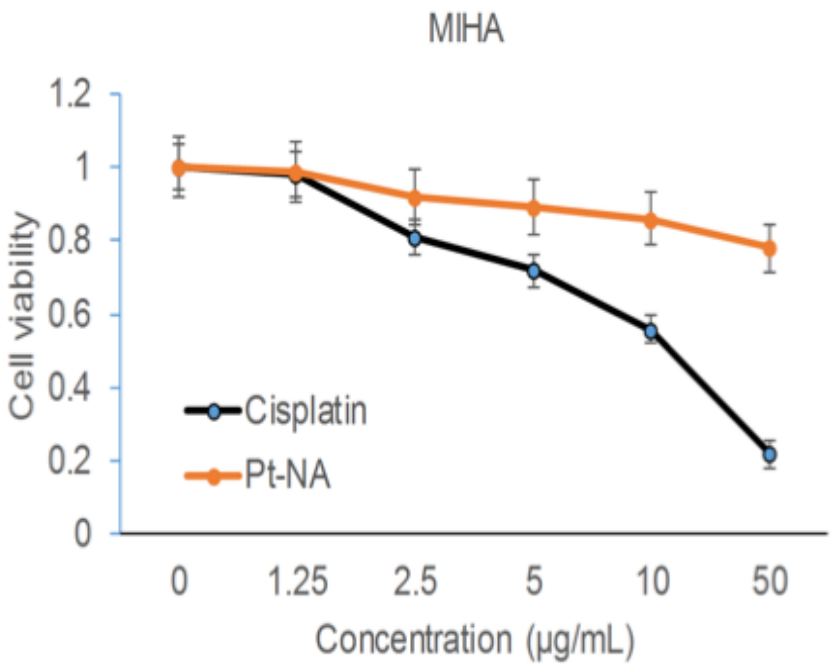

Figure S18. Dose-dependent inhibition effects of Pt-NA and cisplatin on cell growth in normal liver cell line MIHA.

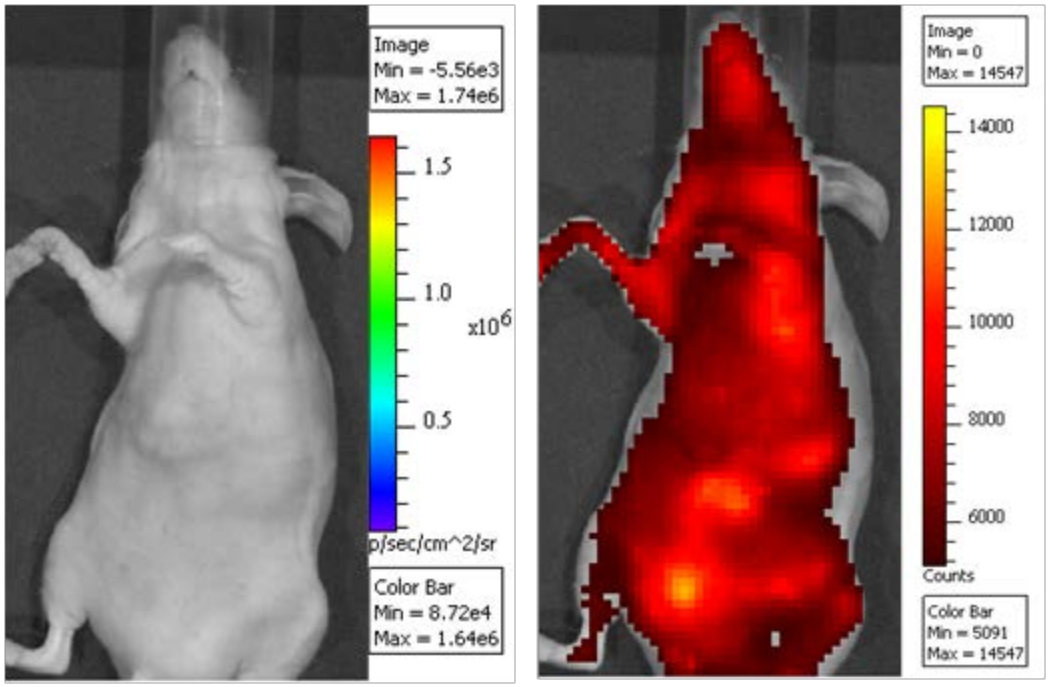

Figure S19. The representative image of IVIS imaging results from a normal nude mouse (with no liver tumor) after Pt-NA injection, which shows relatively random distribution in the different organs.

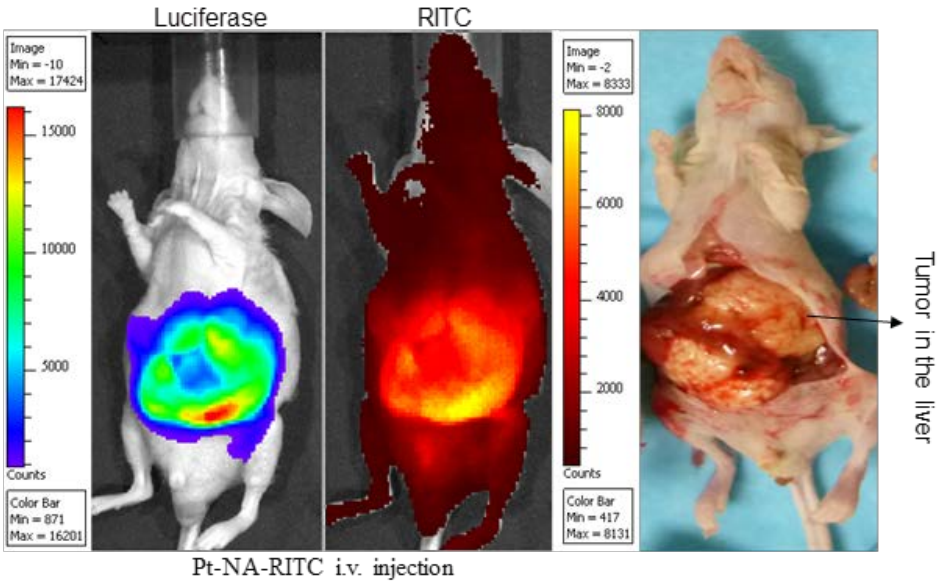

Figure S20. The representative image of IVIS imaging results from a HCC mouse model (with orthotopic liver tumor) after Pt-NA injection, which shows tumor accmulation effect. The luciferase signal shows the orthotopic xenograft tumor and the RITC signal shows the Pt-NA accmulation effect. The right image is the big orthotopic xenograft tumor in the liver after resection.

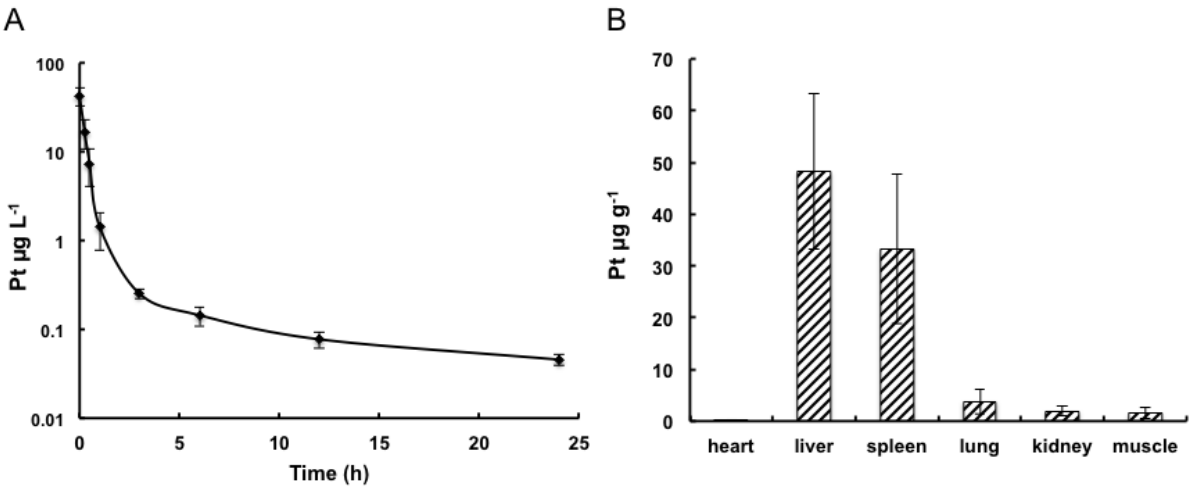

Figure S21. (A) Time profiles of Pt concentration in balb/c mice after a single i.v. injection of Pt-NA (n=6). Values are shown as means ± SD. (B) Tissue distribution of Pt 24 h after a single i.v. injection of Pt-NA in normal balb/c mice (n=6). Values are shown as means ± SD.

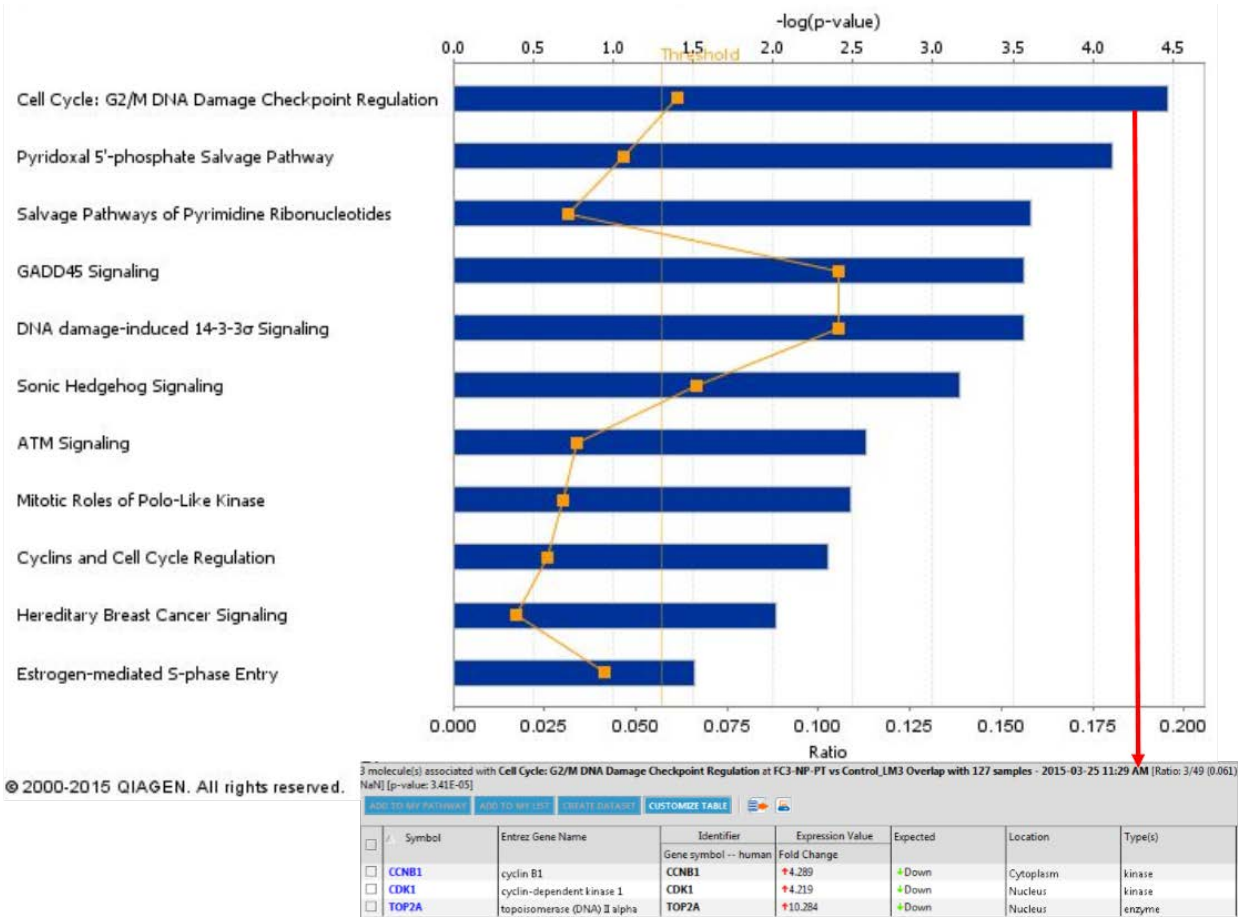

Figure S22. Ingenuity pathway analysis (IPA) demonstrates the down-regulation of genes highly expressed in HCC patient samples by Pt-NA. The threshold line corresponds to a p-value of 0.05 in IPA. The red arrow represents the upregulated fold change of these genes in our patients' HCC samples. These genes were downregulated by Pt-NA as shown the green arrow.

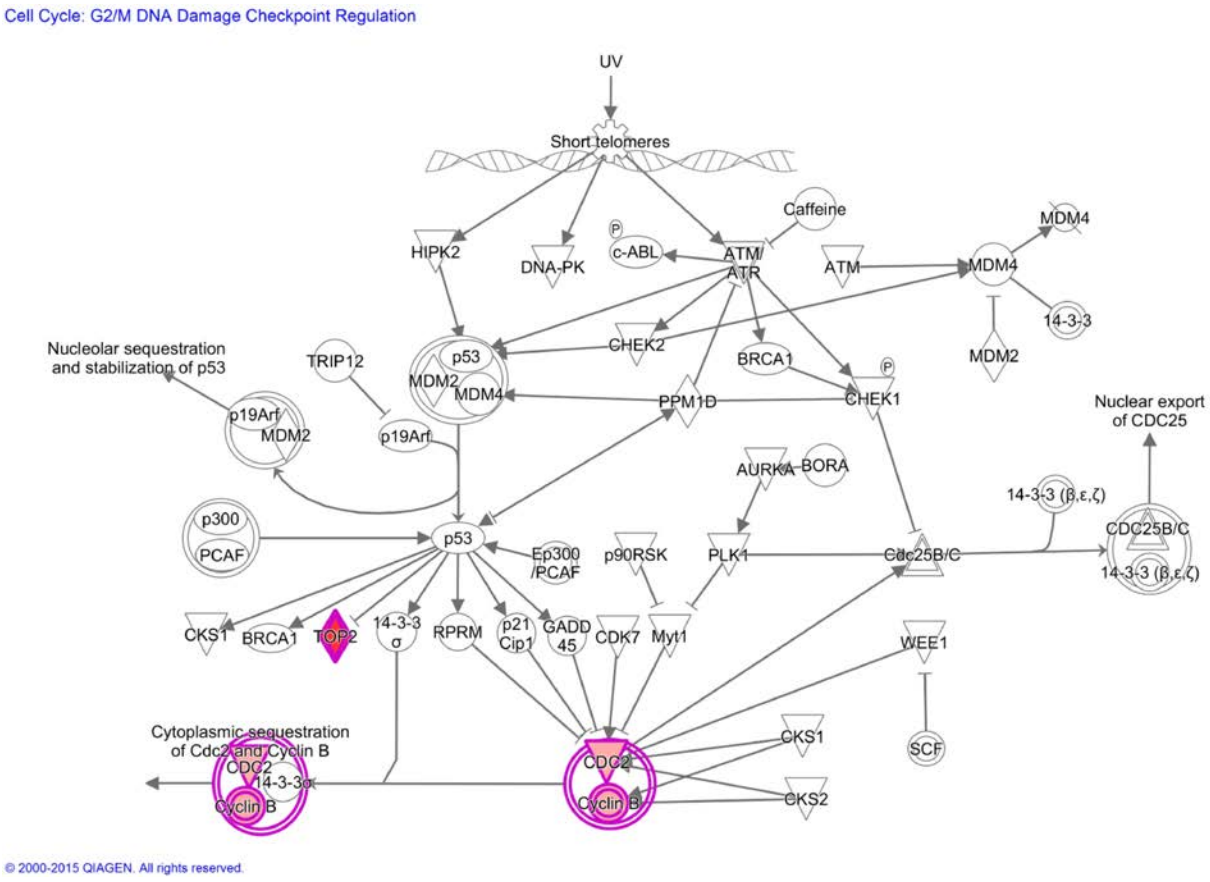

Figure S23. Pt-NA downregulates *CCNB1*, *CDK1* and *TOP2A* and modulates cell cycle G2/M DNA damage regulation by ingenuity pathway analysis.

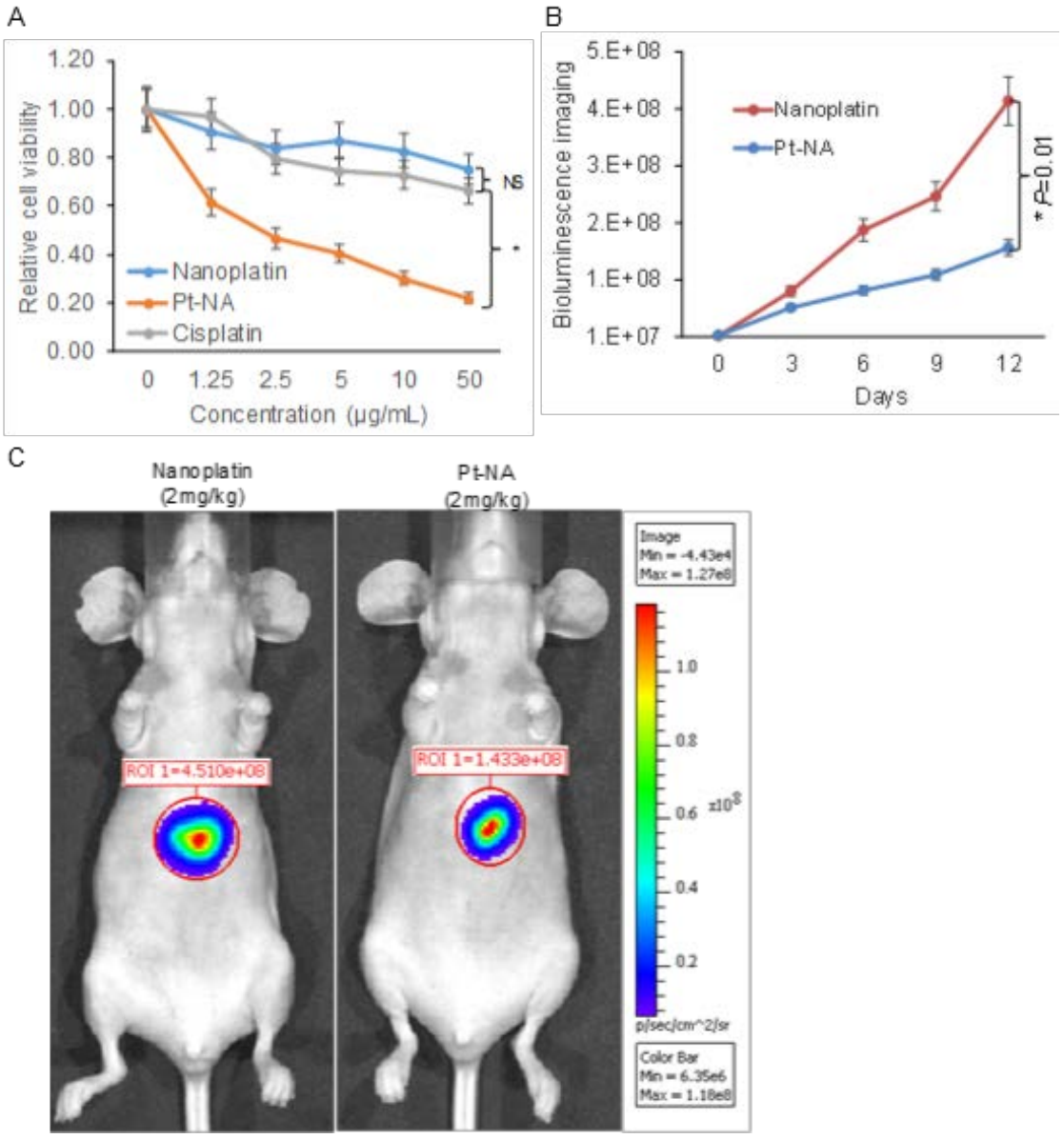

Figure S24. The *in vitro* and *in vivo* anti-tumor efficacy of Pt-NA compared to cisplatin incorporating polymeric micelles (Nanoplatin). (A) The cell viability experiment showed CSLCs of HCC are much more sensitive to Pt-NA than that of Nanoplatin and Cisplatin. (B) The tumor growth curve showed that Pt-NA is significantly better tumor inhibition efficacy than Nanoplatin. (C) Representative images showing bioluminescence signals of the orthotopic tumor xenografts at the therapeutic endpoint of Pt-NA and Nanoplatin treatments.

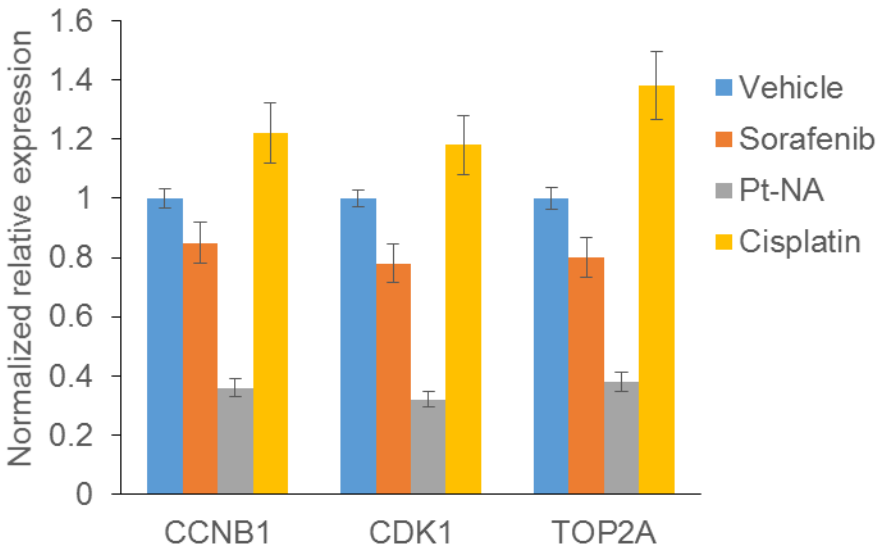

Figure S25. The expression of *CCNB1*, *CDK1* and *TOP2A* in the different treatment tumor tissues was examined by real time RT-qPCR. The results indicate that the expression of *CCNB1*, *CDK1* and *TOP2A* in the tumor tissues significantly decreased by the treatment with Pt-NA, but not in the tumor tissues treated with sorafenib or cisplatin.

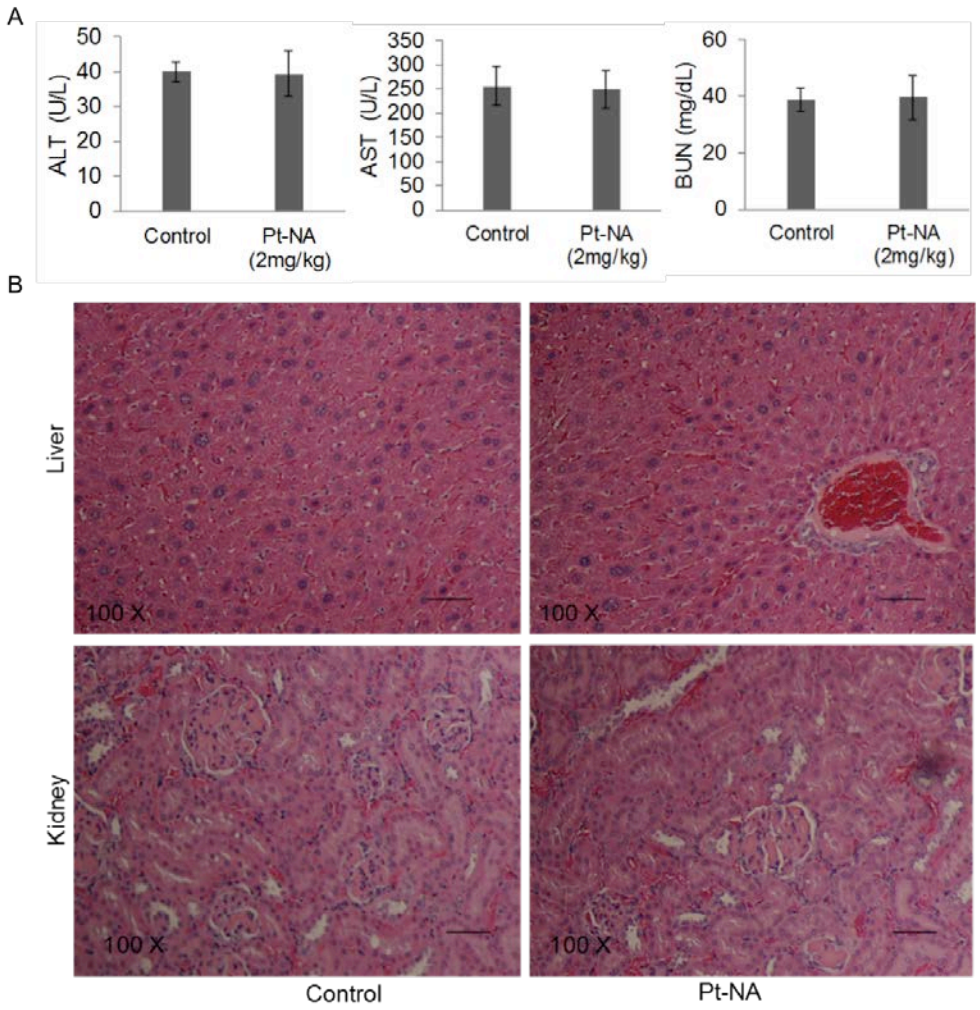

Figure S26. The liver and renal toxicity of the Pt-NA: (A) by detecting the level of ALT (alanine transaminase) and AST (aspartate transaminase) [for liver function] and BUN (blood urea nitrogen) [for kidney function] level in the blood, indicating that Pt-NA has neither increased toxicity nor any significant effects on the level of ALT, AST and BUN in mice. (B) histopathological examination of mice liver and kidney, which shows no toxicity of Pt-NA. (Scale bar, 100 μm)

Table S1. Pt-NA induces downregulation of many liver cancer high expression genes.

Probeset ID	Gene Symbol	Fold-Change (T vs. MN) [a]	Fold-Change (Pt-NA vs. NC) [b]
222608_s_at	ANLN	5.89787	-2.18781
219918_s_at	ASPM	7.51528	-2.35768
209642_at	BUB1	3.14716	-2.18256
203755_at	BUB1B	4.2964	-2.0197
214710_s_at	CCNB1	4.28876	-2.16991
208650_s_at	CD24	3.58646	-2.75035
203213_at	CDK1	4.21852	-2.36039
222848_at	CENPK	3.10056	-2.72297
218585_s_at	DTL	4.81131	-3.30131
219990_at	E2F8	3.09197	-2.30187
219787_s_at	ECT2	4.32835	-2.01192
225687_at	FAM83D	3.72696	-2.13604
206102_at	GINS1	4.09055	-2.74074
227350_at	HELLS	3.26035	-4.15182
202503_s_at	KIAA0101	3.54018	-2.51463
218755_at	KIF20A	3.82143	-2.40323
203362_s_at	MAD2L1	3.65102	-3.39711
218883_s_at	MLF1IP	3.57751	-2.66713
218662_s_at	NCAPG	3.60241	-2.80372
204162_at	NDC80	3.63725	-2.30081
204641_at	NEK2	5.1595	-2.01341
219148_at	PBK	4.79439	-2.82619
204146_at	RAD51AP1	3.20751	-2.69146
201291_s_at	TOP2A	10.2845	-2.04606
204822_at	TTK	3.28556	-2.52939
225655_at	UHRF1	3.75365	-2.31987

[a] The change of genes in Tumor vs Matched Normal HCC patients' samples.

[b] The change of genes in sorted CSLCs treated with Pt-NA vs. VC (Vehicle Control).

REFERENCES

(1) Ling, D.; Park, W.; Park, S.-j.; Lu, Y.; Kim, K. S.; Hackett, M. J.; Kim, B. H.; Yim, H.; Jeon, Y. S.; Na, K.; Hyeon, T. Multifunctional tumor pH-sensitive self-assembled nanoparticles for bimodal imaging and treatment of resistant heterogeneous tumors. *J. Am. Chem. Soc.* **2014**, *136*, 5647-5655.

(2) Ling, D.; Xia, H.; Park, W.; Hackett, M. J.; Song, C.; Na, K.; Hui, K. M.; Hyeon, T. pH-sensitive nanoformulated triptolide as a targeted therapeutic strategy for hepatocellular carcinoma. *ACS Nano* **2014**, *8*, 8027-8039.

(3) Wu, B.; Dröge, P.; Davey, C. A. Site selectivity of platinum anticancer therapeutics. *Nat. Chem. Biol.* **2008**, *4*, 110-112.

(4) Kikuchi, Y.; Miyauchi, M.; Kizawa, I.; Oomori, K.; Kato, K. Establishment of a cisplatin-resistant human ovarian cancer cell line. *J. Natl. Cancer Inst.* **1986**, *77*, 1181-1185.

(5) Hong, W. S.; Saijo, N.; Sasaki, Y.; Minato, K.; Nakano, H.; Nakagawa, K.; Fujiwaka, Y.; Nomura, K.; Twentyman, P. R. Establishment and characterization of cisplatin-resistant sublines of human lung cancer cell lines. *Int. J. Cancer* **1988**, *41*, 462-467.

(6) Xia, H.; Chen, J.; Shi, M.; Gao, H.; Sekar, K.; Seshachalam, V. P.; Ooi, L. L. P. J.; Hui, K. M. EDIL3 is a novel regulator of epithelial-mesenchymal transition controlling early recurrence of hepatocellular carcinoma. *J. Hepatol.* **2015**, *63*, 863-873.

(7) Xia, H.; Ooi, L. L. P. J.; Hui, K. M. MicroRNA-216a/217-induced epithelial-mesenchymal transition targets PTEN and SMAD7 to promote drug resistance and recurrence of liver cancer. *Hepatology* **2013**, *58*, 629-641.